Appl. Phys. B 65, 419–421 (1997)

Applied Physics B Lasers and Optics

© Springer-Verlag 1997

Rapid communication

Nanoscale atomic lithography with a cesium atomic beam

F. Lison[1], **H.-J. Adams**[1], **D. Haubrich**[1], **M. Kreis**[1], **S. Nowak**[2], **D. Meschede**[1]

[1] Institut für Angewandte Physik, Universität Bonn, Wegelerstr. 8, D-53115 Bonn, Germany
(Fax: +49-228/733474, E-mail: sek@iap.uni-bonn.de)
[2] Fakultät für Physik, Universität Konstanz, Universitätsstr. 10, D-78457 Konstanz, Germany

Received: 3 July 1997/Accepted: 7 July 1997

Abstract. We have demonstrated the lithographic production of a periodic nanostructure by focusing a transversely laser cooled cesium atomic beam with a standing-wave light field. With a self-assembled monolayer used as the resist on a gold surface, exposure to cesium atoms locally changes the wetability. Subsequently a wet-etching process transfers the pattern to the underlying gold film. We have generated lines with a separation of half the wavelength of the cesium D_2 line (852 nm) and a width of about 120 nm and covering a large area of approximately 1 mm^2.

PACS: 32.80.Pj; 42.50.Vk; 42.82.Cr; 85.40.Ux

In order to meet future demands for nanofabrication, lithographic processes with sub-100-nm resolution are required. Atoms with a velocity of several tens of meters per second have de Broglie wavelengths in the picometer regime and hence diffraction does not prevent the focusing of atomic beams to a nanometer spot size. Atomic beams are therefore a natural candidate for generating nanostructures, a field called atom lithography. Previously a direct writing process, by focusing an atomic beam with a standing-wave light field into narrow lines spaced by half the optical wavelength, has been demonstrated for sodium [1], chromium [2, 3], and aluminum [4].

In a different approach, the workhorses of laser cooling and atom optics, cesium [5, 6] and metastable argon and helium atoms [7, 8] have been used to structure a gold layer in a resist-based process using a contact mask. We demonstrate a lithographic process that combines the advantages of both techniques: a perfect nonmaterial mask and a nonlinear exposure process which leads to nearly background-free structures.

1 Physical principle

An inhomogeneous light field exerts a force on neutral atoms. This force is due to the interaction of the induced atomic dipole moment with the inhomogeneous electric field. If the frequency of the electric field is near an atomic resonance the dipole force is resonantly enhanced and laser intensities of a few mW/cm^2 are sufficient to manipulate atomic trajectories.

However, to avoid spontaneous emission laser detuning, $\delta = \nu_{\text{laser}} - \nu_{\text{atom}}$, much larger than the natural linewidth γ of the atomic resonance is necessary. In this case the force on the atoms can be written as [9]

$$\boldsymbol{F} = -\frac{h\gamma^2}{8\delta I_{\text{sat}}} \nabla I(\boldsymbol{x}) , \tag{1}$$

where I_{sat} is the saturation intensity of the atomic transition.

In a one-dimensional standing-wave light field with wavelength $\lambda = 2\pi/k$ the intensity pattern is given by $I = I_0 \sin^2(kx)$. If the laser frequency is larger (smaller) than the frequency of the atomic resonance the force on the atoms is directed towards the intensity nodes (antinodes). A Taylor expansion of the force in (1) yields harmonic binding to modal planes. Therefore the standing-wave light field acts as an array of cylindrical lenses for a traversing atomic beam and the atoms are focused into lines with a separation of half the wavelength used (Fig. 1). We used the cesium D_2 resonance at $\lambda = 852.1$ nm with a saturation intensity of $I_{\text{sat}} = 1.1$ mW/cm^2 and a natural linewidth of $\gamma = 5.22$ MHz.

2 Experimental setup

Our beam source is a thermal cesium atomic beam (oven temperature $T = 410$ K) which is geometrically collimated to about 5 mrad (Fig. 2a). Further reduction of divergence to improve the imaging properties of the light lenses is accomplished by two-dimensional transverse laser cooling (Fig. 2b) with two diode lasers at 852 nm. The two laser beams are superimposed, coupled into one optical fiber, and guided to the vacuum apparatus. The cooling laser ($P = 22$ mW, $I = 8\, I_{\text{sat}}$) is detuned by -14 MHz from the $^2S_{1/2} \rightarrow {}^2P_{3/2}$, $F = 4 \rightarrow F' = 5$ cooling transition of the cesium D_2 line, and the second laser ($P = 220\,\mu$W) is tuned to the $F = 3 \rightarrow F' = 4$ resonance and empties the statistically populated

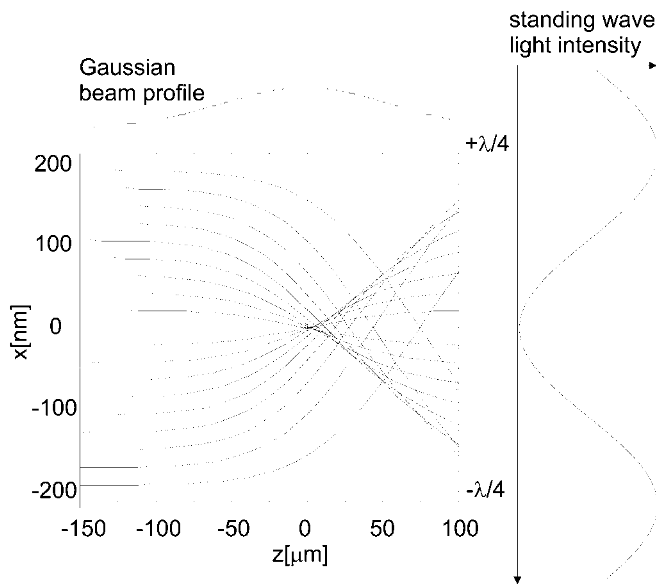

Fig. 1. Calculated atomic trajectories in one period ($\lambda/2$) of a transverse standing-wave light field. The atomic beam is assumed to be monoenergetic with $v_z = 300$ m/s, the most probable atomic velocity of the atomic beam and perfectly collimated. The parameters, $\lambda = 852.1$ nm, $P = 160$ mW, and $\delta = +12.1$ GHz, of the optical standing wave used in the calculation match the experimental situation. On top, the Gaussian beam profile of the standing-wave light field in the direction of propagation of the atomic beam is shown. The vertical line at $z = 0$ indicates the position of the sample

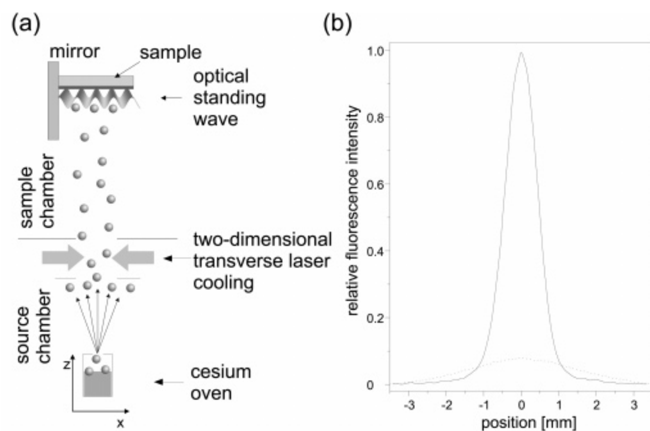

Fig. 2. a Sketch of the experimental setup housed in a high-vacuum apparatus showing cesium beam source, two-dimensional optical collimation stage (source chamber), standing-wave light field, and sample (sample chamber). **b** Beam profiles of the atomic beam with (*solid line*) and without (*dotted line*) two-dimensional optical transverse collimation. The beam profiles were taken with a CCD camera 1 m beyond the collimation stage where the atoms traverse a resonant laser beam

$F = 3$ ground state. In a lin $\perp$ lin polarization configuration [10] the collimation stage increases the total flux through the aperture above by a factor of three, leading to a flux of 10^{12} atoms/cm^{-2}s^{-1} in the sample region. The remaining divergence is less than 0.4 mrad, which corresponds to a transverse energy of 11 neV.

The setup for the standing-wave light field used for focusing of the atomic beam is housed in a second vacuum chamber connected to the source chamber (Fig. 2a). A highly reflecting mirror is aligned parallel (± 0.2 mrad) and in close vicinity (< 1 mm) to the atomic beam axis. Two 90° prisms attached to the mirror surface on both sides of the atomic beam serve as the sample holder and guarantee the right-angle between sample surface and atomic beam axis.

The standing-wave light field is derived from a Ti:Sapphire laser beam, which is also led to the vacuum apparatus via an optical fiber. The well-collimated laser beam, with a diameter (e^{-2}) of 1.4 mm, is focused with a cylindrical lens ($f = 250$ mm), placed outside the vacuum chamber, onto the mirror surface, resulting in a waist of 100 μm in the direction of the atomic beam (z axis). A maximum laser power of 160 mW is available for the standing wave light field. We adjust the standing wave light field perpendicular to the mirror surface by optimizing the retroreflection into the optical fiber. The sample surface is placed in the center of Gaussian beam profile. A detuning of $+12.1$ GHz with respect to the $F = 4 \rightarrow F' = 5$ transition was chosen according to the simulation of the atomic trajectories in order to achieve focusing for the most probable velocity (300 m/s) within the cesium beam (Fig. 1). The parameters given above result in a potential depth of 620 neV, which is much larger than the remaining transverse kinetic energy of the atomic beam.

Sample preparation was carried out according to the procedure described in [8]. A polished silicon wafer with a 1 nm chromium layer is coated with a 30-nm gold layer. Immediately after evaporation of gold these samples are immersed into a 1-mM solution of nonanethiole [$CH_3(CH_2)_8SH$] in ethanol for at least 24 hours. During that time an approximately 1-nm thick self-assembling monolayer (SAM) of nonanethiole is formed [11] (Fig. 3). The hydrophobic character of the methyl end groups protects the underlying gold surface during a wet gold etching process. The exposure of the SAM to cesium atoms locally changes the hydrophobic property [5, 6]. A dose of about eight cesium atoms per nonanethiole molecule, which corresponds to approximately 4×10^{15} cesium atoms cm^{-2} was found to be sufficient. The portion of cesium dimers in the atomic beam, which is less than 0.1% [12], is neglected, though it is not yet clear whether they damage the SAM as well. After exposure to the cesium atomic beam for four to ten minutes at a background pressure of about 10^{-8} mbar, the samples were etched in the gold etching solution [13] for 11 min. No special care was taken to protect the samples from environmental contamination during the preparation and etching process.

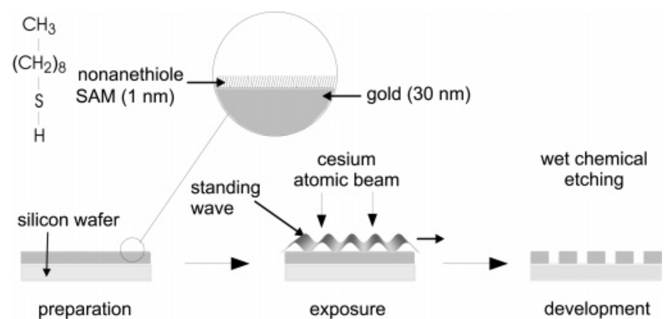

Fig. 3. The lithographic process consists of sample preparation, structuring the resist with a cesium atomic beam, and etching in a gold etching solution

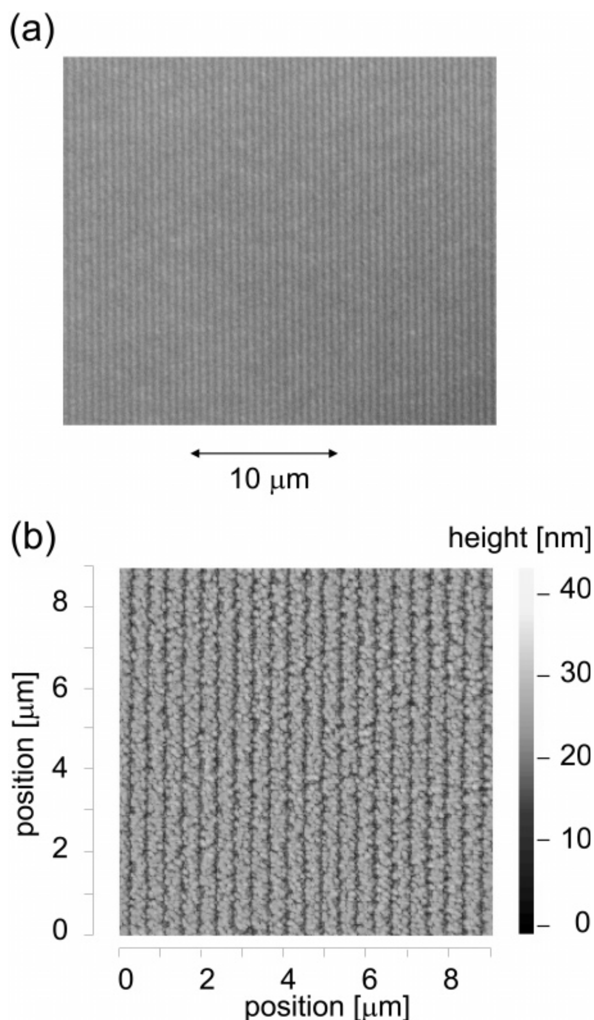

Fig. 4a,b. Microscopic images of the written structures. In both images, bright structures represent areas of gold, silicon is dark. **a** Light microscope image using difference interference contrast. These lines can be found in the whole region exposed to the atomic beam with a diameter of 1 mm. **b** Atomic force microscope image of a region (9 μm × 9 μm) scanned in contact mode

3 Discussion of results

Optical microscopy is well suited for obtaining a general overview of the developed samples. In the difference interference contrast image (Fig. 4a) the lines written in the gold layer are clearly visible and the ratio between the ditch and bridge widths can be estimated. The lines were written in the entire area exposed to the atomic beam (Ø = 1 mm). Using the samples as a grating allows the period of the lines to be determined. In a Littrow setup we measured an angle of incidence of 47.9(1)° for the −1st diffraction order of a helium–neon laser beam at 632.8 nm, which corresponds to a periodicity of 426.4(7) nm [2 347 (6) lines/mm]. For a more quantitative analysis we inspected the samples by means of an atomic force microscope (AFM, from Zeiss). After calibration of the AFM with a length standard produced by e-beam lithography (uncertainty less than 1%), we determined the line separation to be 425 (4) nm. In underexposed samples we find connections between the lines, whereas in overexposed samples the lines show disconnections. The best results were obtained at an exposure time of 6 min. For an unfocused but collimated atomic beam this exposure time would be too low by a factor of three. The measured averaged linewidth of the lines of about 120 nm agrees quite well with this ratio.

The lithographic process described is very robust and reliable because of the use of a low-temperature cesium source. The combination of the high flux and low dose leads to short exposure times of less than 10 min, which can easily be reduced by increasing the oven temperature. The current linewidth is mainly limited by the isotropic gold etch process and the graininess of the gold film used, which we believe is due to the layer-plus-island growth mode (Stranski–Krastanov) of gold on silicon [14]. This limitation can for instance be overcome by using a different resist based on alkylsiloxanes [$CH_3(CH_2)_nSiCl_3$] on silicon dioxide, which was found to be sensitive to cesium atoms too [15]. The method described can be extended straightforwardly into two dimensions as has already been shown for chromium [16, 17], or may be combined with magnetic imaging [18] in order to produce an arbitrary complex structure.

Atom lithography has several advantages. We have demonstrated that it can be used to modify suitable surfaces at nanometer scales in a manner similar to traditional print and lift-off techniques. It is highly parallel and the intrinsic interferometric control of the length scales during exposure may be useful for the fabrication of submicron length standards.

Acknowledgements. Financial support from the BMBF is much appreciated. The charges for our cesium oven were provided by CHEMETALL GmbH, Frankfurt a. M.

References

1. G. Timp, R.E. Behringer, D.M. Tennant, J.E. Cunningham, M. Prentiss, K.K. Berggren: Phys. Rev. Lett. **69**, 1636–1639 (1992)
2. J.J. McClelland, R.E. Scholten, E.C. Palm, R.J. Celotta: Science **262**, 877–880 (1993)
3. U. Drodofsky, J. Stuhler, B. Brezger, T. Schulze, M. Drewsen, T. Pfau, J. Mlynek: Microelectronic Engineering **35**, 285–288 (1997)
4. R.W. McGowan, D.M. Giltner, S.A. Lee: Opt. Lett. **20**, 2535 (1995)
5. M. Kreis, F. Lison, D. Haubrich, S. Nowak, T. Pfau, D. Meschede: Appl. Phys. B **63**, 649–652 (1996)
6. K.K. Berggren, R. Younkin, E. Cheung, M. Prentiss, A. Black, G.M. Whitesides, D.C. Ralph, C.T. Black, M. Tinkham: Adv. Mat. **9**, 52 (1997)
7. K.K. Berggren, A. Bard, J.L. Wilbur, J.D. Gillaspy, A.G. Helg, J.J. McClelland, S.L. Rolston, W.D. Phillips, M. Prentiss, G.M. Whitesides: Science **269**, 1255 (1995)
8. S. Nowak, T. Pfau, J. Mlynek: Appl. Phys. B **63**, 203–205 (1996)
9. J. Dalibard, C. Cohen-Tannoudji: J. Opt. Soc. Am. B **2**, 1707–1720 (1985)
10. D.S. Weiss, E. Riis, Y. Shevy, P.J. Ungar, S. Chu: J. Opt. Soc. Am. B **6**, 2072–2083 (1989)
11. A. Ulman, *Ultrathin Organic Films* (Academic Press, Boston, MA 1991)
12. A.N. Nesmeyanov, *Vapor Pressure of the Chemical Elements* (Elsevier, Amsterdam 1963)
13. Y. Xia, X.-M. Zaho, E. Kim, G.M. Whitesides: Chem. Mater. **7**, 2332 (1995)
14. H. Lüth, *Surfaces and Interfaces of Solid Materials* (Springer, Berlin, Heidelberg 1995)
15. R. Younkin, K.K. Berggren, K.S. Johnson, D.C. Ralph, M. Prentiss, G.M. Whitesides: submitted to Appl. Phys. Lett.
16. R. Gupta, J.J. McClelland, Z.J. Jabbour, R.J. Celotta: Appl. Phys. Lett. **67**, 1378–1380 (1995)
17. U. Drodofsky, J. Stuhler, T. Schulze, M. Drewsen, B. Brezger, T. Pfau, J. Mlynek: Appl. Phys. B, to be published
18. W.G. Kaenders, F. Lison, A. Richter, R. Wynands, D. Meschede: Nature **375**, 214–216 (1995)